Experiments in Fluids 32 (2002) 417–424 © Springer-Verlag 2002
DOI 10.1007/s003480100355

Digital compensation of pressure sensors in the time domain

G. Paniagua, R. Dénos

Abstract This contribution presents an innovative technique to determine the transfer function of pneumatic and fast-response pressure probes. The dynamic response is determined experimentally with pressure step-tests. In the case of conventional instrumentation fast-opening valves or balloon explosions are used. For the fast-response pressure sensors, shock tube tests are performed. The response of the probe is fitted in the time domain with the response of an *m*-order linear system. This numerical system is then used to correct the lag and dynamic error of the measurement chain.

1 Introduction

A fundamental concern for the experimentalist is to ensure a sufficiently fast response of the probes to cope with the range of frequencies existing in a fluctuating flow. In turbomachinery applications, unsteadiness exhibits a wide frequency spectra (from a few Hz to 30 kHz) either attributed to the way the machine is operated (e.g. transient flow conditions such as those encountered in short-duration facilities), or to turbomachine instabilities (combustor-induced inlet distortion, rotating stall, surge and blade row interference effects). However, due to cost, manufacturing and aerodynamic constraints, it is not always possible to guarantee a high-frequency response of the probe.

In the past, researchers have corrected the lag in the response of thermocouples, associated to unsteady heat transfer phenomena directly linked to the size of the bead diameter, using electronic compensator circuits, as explained by Warshawsky (1991). The advantages of digital methods are obvious: no additional hardware, less cost. Additionally, digital procedures are flexible techniques that can be adapted easily to changes in testing conditions (time constants of thermocouples depend on the Reynolds number of the flow under investigation). A recent example in the literature of a simple first-order system is a model proposed by Redionitis and Pathak (1999) for straight tubing assemblies in pressure probes, but it is only valid for over-damped or critically damped systems. Dénos and Sieverding (1997) elaborated a more advanced procedure to correct the response of cold wires and thermocouples. The method uses a combination of *n* first-order systems to compensate both the unsteady conduction between the thin wire and its supports and the lack of response of the wire at high frequency.

In general, combinations of first-order systems cannot model pressure tube response. The present contribution describes a digital procedure to determine the dynamic response of the pressure measurement chain using an *m*-order linear system model. This system is discrete because data is acquired at a certain sampling frequency f_s. Let us consider as input of the digital system the *true* flow pressure $\{u_k\}$ and as output what the measurement chain delivers, $\{y_k\}$. The first objective is to determine the parameters that model the transfer function of this system (see Fig. 1, 'TF Identification'). The method presented hereafter is based on the general recursive least squares algorithms described in detail by Issermann (1981). The method allows the determination of the parameters of the transfer function in real time. However, in our particular application to short-duration facilities, a post-processing routine is more suitable, because the tests last for less than a second and the parameters are not expected to change during the running time. Therefore, a direct least squares algorithm was implemented.

The second step in the data reduction procedure, called 'digital compensation' in Fig. 1, consists in the determination of the corrected measurements $\{\hat{u}_k\}$, using the inverse transfer function.

The above-described method had been evaluated and is currently in use at the Von Karman Institute (VKI) for correcting conventional pressure measurements, in order to extend their frequency bandwidth. The effectiveness of the method is demonstrated through several examples.

2 Digital system identification methods

2.1 Parametric system identification methodology

To evaluate digitally the transfer function, there are parametric methods or non-parametric procedures such as the fast Fourier transform (FFT), described in detail by

Received: 27 November 2000 / Accepted: 4 July 2001

G. Paniagua (✉), R. Dénos
Von Karman Institute for Fluid Dynamics
72 Chaussée de Waterloo
1640 Rhode St Genése, Belgium

The authors wish to thank M. Kinnaert (Professor at Université Libre de Bruxelles) and H. Lopez Garcia (Professor at Universidad de Oviedo) for their advice. Likewise, the authors wish to thank N. Billiard and M. Sardina for their efforts in the development of the procedure. Finally, many thanks to J.M. Desse (Onera IMFL, France) for his assistance in the shock tube tests.

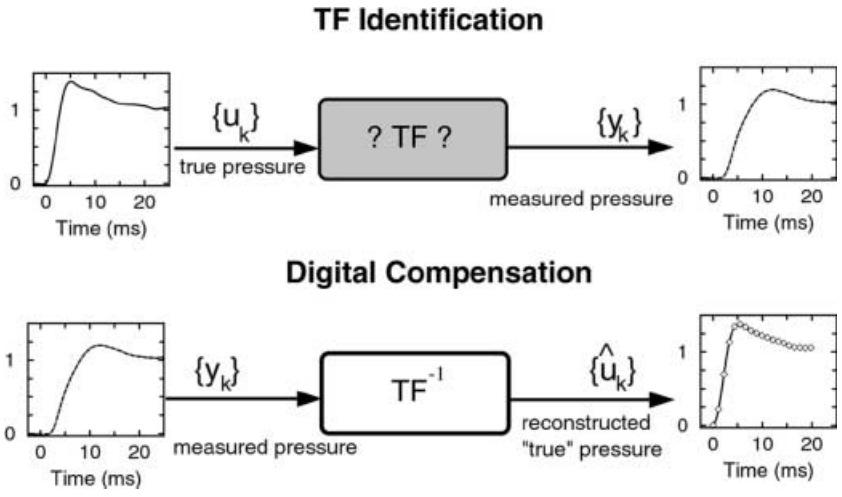

Fig. 1. Discrete model of the measurement chain

Press et al. (1986). With the conventional FFT technique, the transfer function is determined in the frequency domain as the ratio between the FFT of the output and the FFT of the input at each frequency. If the signals are sampled at $N = 2^p$ instants, the transfer function is a set of $N/2$ complex numbers. In contrast, a parametric method only requires few parameters to be stored, compared to the FFT.

The FFT requires periodic excitations to be free of errors, which is an important constraint in its use. In the case of a rising step test, the step signal can be converted into a periodic function by imposing the signal to return to its initial level before the test, e.g. through an inverted step or a sinusoidal decrease (Popp 1999). Gossweiler (1993) solves the problem by performing derivatives of the signals before computing the FFT.

Another concern is the Gibbs phenomenon, discussed extensively by Canuto et al. (1991). There is a characteristic oscillatory behaviour of the FFT in the neighbourhood of the step with an overshoot and alternating local minima and maxima. The overshoot tends toward the point of discontinuity as the number of retained frequencies is increased. Due to this unavoidable problem, the FFT ratio between the perfect step (input data) and the measurement chain output is not correct. Thus, the reconstructed signal can never be the '*true*' pressure.

Parametric methods in the time domain avoid the previous two problems. There is a wide number of techniques to estimate parameters: maximum likelihood, least squares, cross-correlation and stochastic approximation. Of all of them, the least squares method offers the simplest concept.

2.2
Direct least squares method

The method assumes that the discrete model (pressure measurement chain) is stable, time invariant and linear, i.e. it can be described by a linear differential equation. The response of most pressure transducers can be represented adequately by solutions of linear differential equations; therefore, their response can be modelled with a linear discrete system of constant coefficients. Bohn and Schnittfeld (1992) showed that non-linear effects in capillary tubes (pneumatic line between the pressure sensor and the measurement location) occur for rather high-pressure amplitude fluctuations leading to shock waves. In presence of temperature gradients, the pressure fluctuation take the form of saw-tooth signals. Schweppe et al. (1963) discuss the analysis of non-linear transducers.

The differential equation of the discrete model can be expressed as an equation in differences (see Eq. 1), in which y_k can be interpreted as a one-step-ahead prediction ${y^{k-1}}_k$ of y_k at time $k-1$.

$$y_k = \sum_{i=0}^{m} b_i \cdot u_{k-i-d} - \sum_{i=0}^{m} a_i \cdot y_{k-i} \qquad (1)$$

The first parameter to determine is T_d, the time delay between the two signals, input and output, which is a characteristic constant of the measurement chain. The corresponding number of samples is $d = f_s \cdot T_d$. In a rising-step test, d is the number of instants for which the output signal remains at 0 level after the input starts rising. Etter (1981) presented two techniques for time delay estimation based on gradient methods and genetics algorithms.

Sometimes it is more practical to work in the Z domain, which is equivalent to the Laplace domain (S) for discrete systems. The Z transform of a time series is $Y(z) = \sum_{k=-\infty}^{\infty} x_k \cdot (z)^{-k}$. Equation 2 expresses the discrete transfer function of a linear system in the discrete Z domain by two polynomials in z, of m-order:

$$\frac{Y(z)}{U(z)} = \frac{b_0 \cdot z^{-d} + b_1 \cdot z^{-1-d} + \cdots + b_m \cdot z^{-m-d}}{1 + a_1 \cdot z^{-1} + a_2 \cdot z^{-2} + \cdots + a_m \cdot z^{-m}} \qquad (2)$$

Nevertheless, for a parametric identification, it is simpler to work in the time domain. It is important to note that the parameters of the transfer function in the Z domain, d, a_i and b_i, are not invariant but depend on the sampling frequency at which the data is sampled. The transfer function is an invariant in the continuous domain S or in the frequency domain.

Since the parameters are obtained from experiments contaminated by noise, it is reasonable to expect some uncertainty. The difference between the one-step-ahead

prediction using the derived parameters and the experimental observed value is the error: $e_k = y_k - y^{k-1}{}_k$.

$$y_k + \hat{a}_1 \cdot y_{k-1} + \hat{a}_2 \cdot y_{k-2} \cdots + \hat{a}_m \cdot y_{k-m} = \hat{b}_0 \cdot u_{k-d} + \cdots + \hat{b}_m \cdot u_{k-d-m} + e_k \quad (3)$$

Because inputs and outputs are measured for $k = 1,2...N$ instants, [N−m−d−1] equations of this type (Eq. 3) can be written. With all the set of Eq. 3 written in matrix form (see Appendix), the experimental trace is expressed as the scalar product of the data matrix Ψ and the parameter vector $\hat{\Theta}$

$$Y_{(m+d+1:N,1)} = \Psi^T_{(m+d:N-1,1:2\cdot m+1)} \cdot \hat{\Theta}_{(2\cdot m+1,1)} + e \quad (4)$$

The algorithm objective is to minimise the quadratic cost function: $\frac{\partial}{\partial \hat{\Theta}} \sum_{k=m+d+1}^{N} (e_k)^2 = 0$, assuming $N \geq 2{\cdot}m$. From this least squares principle the expression of the parameter vector is derived:

$$\hat{\Theta}_{(2\cdot m+1,1)} = P_{(2\cdot m+1,2\cdot m+1)} \cdot \Psi_{(1:2\cdot m+1,m+d:N-1)} \cdot Y_{(m+d+1:N,1)}$$
$$P_{(2\cdot m+1,2\cdot m+1)} = \left[\Psi_{(1:2\cdot m+1,m+d:N-1)} \cdot \Psi^T_{(m+d:N-1,1:2\cdot m+1)} \right]^{-1} \quad (5)$$

Finally, when the parameters are determined, Bode plots can be obtained using Eq. 2 and the definition of z in the frequency domain $z = e^{j\cdot 2\pi\cdot f/f_s}$. With the following set of Eq. 6, the transfer function modulus and the phase can be computed at any frequency:

$$\begin{aligned} |Y(f)/U(f)| &= \sqrt{(l_1^2 + l_2^2)/(h_1^2 + h_2^2)} \\ \phi &= a\tan(l_2/l_1) - a\tan(h_2/h_1) \\ l1 &= \sum_{i=0}^{m} b_i \cdot \cos[2 \cdot \pi \cdot f/f_s \cdot (-i-d)] \\ l2 &= \sum_{i=0}^{m} b_i \cdot \sin[2 \cdot \pi \cdot f/f_s \cdot (-i-d)] \\ h1 &= 1 + \sum_{i=1}^{m} a_i \cdot \cos[2 \cdot \pi \cdot f/f_s \cdot (-i)] \\ h2 &= \sum_{i=1}^{m} a_i \cdot \sin[2 \cdot \pi \cdot f/f_s \cdot (-i)] \end{aligned} \quad (6)$$

When the transducer is well calibrated in the steady state, it is verified that, at zero frequency, the gain is equal to 1: $\sum_{i=0}^{m} b_i / \left(1 + \sum_{i=1}^{m} a_i\right) = 1$. The determination of the transfer function in the frequency domain or in the S domain is useful, because it is an invariant of the system, independent of the sampling frequency. When the sampling frequency varies, the parameters of the digital transfer function change. Firstly, the new delay is $d_2 = T_d/f_{s2}$. Then, the transfer function in the frequency domain is used to obtain the new parameters for a different sampling frequency, going from the frequency domain back to the Z domain.

The computational effort to determine the transfer function is lower using FFT (see left side of Fig. 2). The FFT requires $N{\cdot}(1{+}p)$ number of floating-point operations, multiplications and additions, while the least squares needs $16{\cdot}m^2{\cdot}N{+}8/3{\cdot}m^3{-}4{\cdot}m^2{-}2{\cdot}m$. However, notice that the transfer function identification is performed only once for each pressure measurement chain.

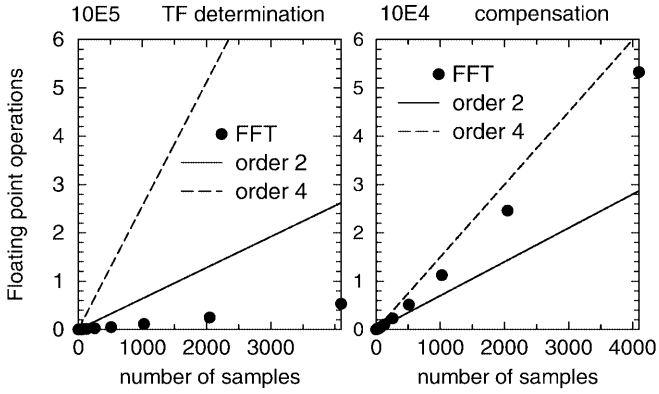

Fig. 2. Computational effort to compute the transfer function and perform the reconstruction of the '*true*' signal

2.3 Digital compensation, reconstruction of the 'true' pressure

It follows from Eq. 4 that the true pressure u_k can be recovered with an iterative process, using the parameters of the transfer function (d, $2{\cdot}m{+}1$ values) and the signal delivered by the pressure measurement chain y_k:

$$\hat{U}_{(m:N-d-1,1)} = Y_{(d+m+1:N,1)} - \Psi^T_{(m+d:N-1,1:2\cdot m)} \cdot \hat{\Theta}_{(2\cdot m,1)} / \hat{b}_1 \quad (7)$$

The initial part of the signal, the first $m{-}1$ instants, for which there is no information, is set by default to what is measured, i.e. $\hat{U}_{(1:m-1,1)} = Y_{(1:m-1,1)}$. There are three steps to compensate, or reconstruct the '*true*' pressure signal using the FFT. First, to transfer the measured signal into the frequency domain (direct FFT), then to divide by the measurement chain transfer function and finally, the '*true*' signal is obtained by inverse FFT. The proposed parametric model is simpler; the reconstruction procedure involves just an iterative multiplication of the measured signal by the measurement chain parameters. In the case of a digital system with order 2 or 3, the parametric model is faster in speed than the FFT (see right side of Fig. 2). FFT requires $N{\cdot}(1{+}p)$ operations, while the least squares method needs $N{\cdot}(4{\cdot}m{-}1)$ calculations.

3 Experimental results

3.1 Experimental dynamic calibration of pressure sensors

Dynamic calibration is the experimental procedure to establish the transfer function between the flow pressure signal '*input*' and the signal supplied by the pressure measurement chain '*output*'. Theoretically, system identification methods require tests that excite all modes of the system.

Since the 1960s the transfer functions of pressure transducers have been determined using various experimental pressure generators: periodic and non-periodic pressure functions. Schweppe et al. (1963) survey many devices used for dynamic calibration methods.

Periodic function generators include acoustical shock generators, rotating wheels with slots (Weyer and Schodl 1971), rotating valves, sirens (Dibelius and Minten 1983), piston in cylindrical devices, electrical and mechanical oscillators. Sinusoidal waves have been used to characterise experimentally pressure lines at different pressure levels (Bergh and Tijdeman 1965). More recently (Boer 1988), boundary layer entrainment effects were also considered in the investigation of pneumatic lines.

Non-periodic pressure functions like pressure steps, however, are in practice advantageous compared to periodic pressure functions, because only one test of short duration is sufficient to cover the entire frequency domain of interest. Quick-acting valves, opening the passage between two chambers that are initially at two different pressures, are suited to generate pressure steps for dynamic calibrations up to 10 kHz (see Pallant 1966 for a complete review of fast-opening valves). The fastest pressure pulses are achieved in a shock tube. A high-pressure chamber is pressurized until a diaphragm bursts, a shock is originated, propagating at the speed of sound along the low-pressure chamber. At the end-wall, the pressure rise is almost a perfect stepwise pressure rise, allowing dynamic calibrations up to and beyond frequencies of 500 kHz. Shock tube tests have recently been used by several researchers to investigate different piezo-resisistive sensors (Ainsworth and Allen 1990) and fast-response aerodynamic probes (Gossweiler et al. 1990). Finally, let us mention the method of Ciocan et al. (1998), who tested the response of their unsteady five-sensor probe in a water tank, where a shock wave is generated by the implosion of a vapour bubble produced with an electrical discharge in the water.

At VKI, three different methods are used for the dynamic testing of pressure probe characteristics. Besides the aforementioned methods of fast-acting valves and shock tubes, VKI developed burst balloons devices. The balloon tests and fast-acting valves were used for the dynamic calibration of pneumatic probes, the shock tube tests for the calibration of the fast-response pressure probes with silicon sensors implemented in the probe head.

3.3 Testing and compensating pneumatic probes and pressure lines

Schemes of the two different burst balloon designs are presented in Fig. 3. In the first design, the pneumatic probe is placed inside of a cylindrical chamber connected to a balloon. In the second design, the probes are directly introduced inside the balloon. In both cases, a pressure line pressurizes a standard plastic balloon to a pressure ranging from 70 to 300 mbar above the atmospheric pressure. When the balloon is exploded, using a needle, the pressure within the chamber or the balloon evolves as a falling-pressure step to atmospheric conditions in ≈700 μs, which allows dynamic calibrations in the range 0–700 Hz. A fast-response Kulite XCQ-062 pressure sensor is placed adjacent to the tested pneumatic probe; the fast-response sensor with a natural frequency around 250 kHz is considered to measure the '*true*' pressure variation.

The first design was developed to test the response of pneumatic five-hole probes. The chamber was intended to protect the probe from the impact of plastic debris. Per contra, the existence of the chamber introduces pressure oscillations of 850 Hz due to reflections of pressure waves in the chamber (see Fig. 4). The amplitudes of the pressure chamber oscillations decrease exponentially. The five sensors of the five-hole probe do not experience these pressure fluctuations because the natural frequency of the line tube-cavity-sensor configuration is far below, around 80 Hz.

The spurious oscillations are eliminated in the second design, with the probes directly immersed in the balloon. The locations of the probes were optimised by a systematic variation of the axial position of the fast-response Kulite sensor inside the balloon. The speed to reach the pressure step is maximum when the balloon is cut at the plane of the axial location of the sensors. To minimise pressure wave reflections, the balloon should be cut at the point of maximum stresses: at the neck. The repeated tests show variations from test to test below 1%.

Both devices are used to dynamically calibrate pneumatic pressure probes used in the large VKI compression tube

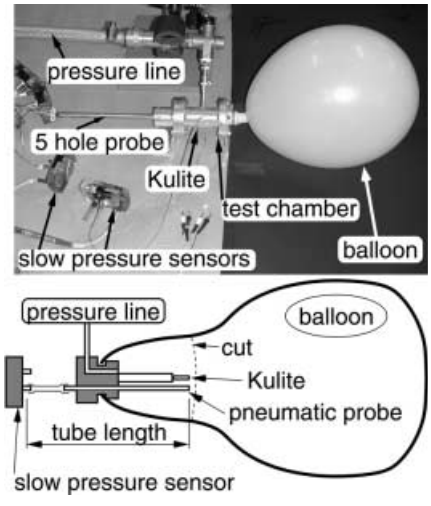

Fig. 3. Set-up of burst-balloon devices

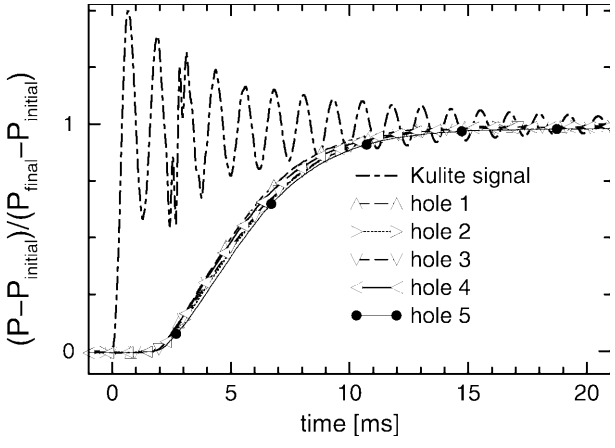

Fig. 4. Five-hole probe step test

facility, a short-duration facility (running time of ≈0.4 s). Tests were performed to characterise the transfer function of capillary tubes of various lengths for static pressure measurements, with diameters of 1.1 mm and 0.7 mm. For all the cases, the sensor cavity is equal to 80 mm^3.

Figure 5 shows some of these tests. In the tests with a tube diameter of 0.7 mm, the signal is always over-damped. For the case of diameter 1.1 mm, the signal is under-damped for lengths above 400 mm, the pressure oscillations are associated with reflections of the pressure fluctuations. In aggressive environments, like measurements in the core of an operating turbine engine, long line probes acting as 'infinite lines' are used to eliminate these pressure reflections (see Coats et al. 1977).

The parameters of the transfer function of each capillary tube are obtained with the direct least squares method. Using Eq. 6, the transfer function modulus and phase can be computed in function of the frequency. Figure 6 plots the natural frequency as a function of the length. The

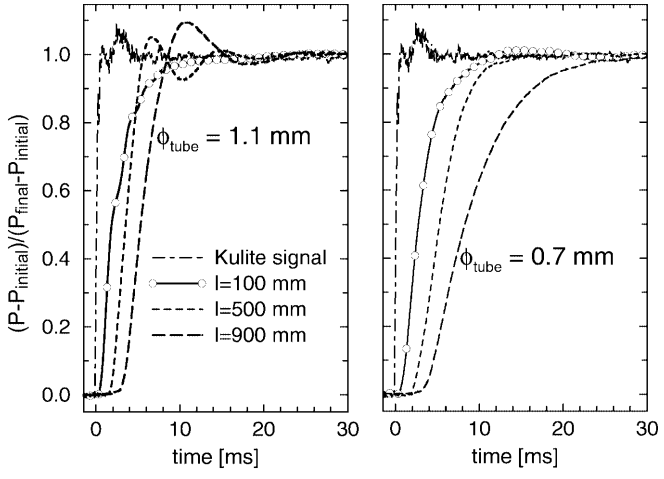

Fig. 5. Effect of the length and the diameter on the time response

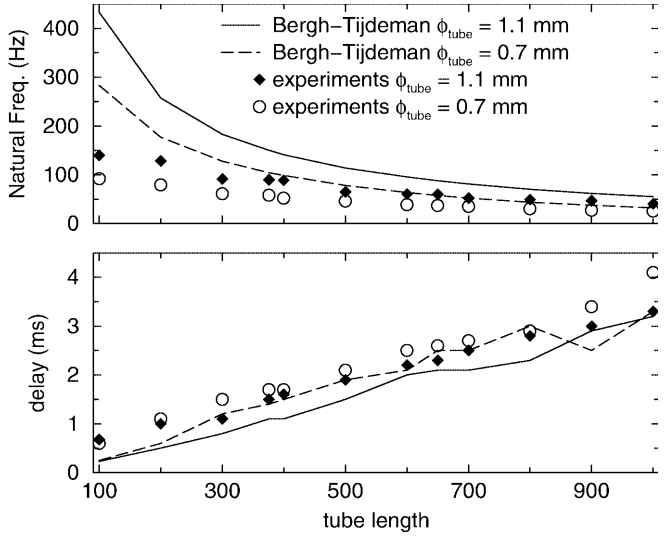

Fig. 6. Effect of the tube length and diameter on the delay and natural frequency

theoretical prediction using the model of Bergh and Tijdeman (1965) over-predicts the natural frequency, probably due to an under-estimation of the sensor cavity. For the 100-mm-length tube, increasing the cavity by 70% yields a reduction in the natural frequency of 19%. In turn, for the tube of 1,000 mm length, the change of natural frequency is only 6%. The time delay is displayed in the lower part of Fig. 6.

Using the transfer function parameters and Eq. 7, the pneumatic probe signal is compensated. In Fig. 7, the fast-response Kulite sensor signal is reproduced by the compensated pneumatic probe signal with high precision. Because the digital compensation utilizes the inverse transfer function, the amplification augments as the frequency increases. Because the compensation amplifies both the high-frequency components of the clean signal and the noise, the accuracy of the compensated signal decreases with increasing frequency. Considering a signal-to-noise ratio of 2%, the maximum amplification amounts to 5 (limiting the noise ratio below 10%), i.e. the minimum gain in the transfer function is 0.2. For the pneumatic signal, the compensation extended the frequency range 3.2 times from 45 Hz up to 146 Hz.

3.3
Blade loss measurements in a short-duration facility with pneumatic pressure probes

The measurement of blade losses in the VKI isentropic light piston compression tube facility with running times of the order of 0.4 s requires probe traversing speeds at about 500 mm/s, i.e. one to two orders of magnitude higher than in conventional continuously running facilities. For example, in the VKI compression tube linear cascade tunnel, the downstream total pressure probe traverses typically 2.5 pitches, i.e. a distance of ≈125 mm, in 0.35 s. The measurements are further complicated by the occurrence of low-frequency (≈20 Hz) total-pressure oscillations with pressure amplitudes of 2–3% of the upstream total pressure. These fluctuations are typical for this type of tunnel. Accurate loss measurements therefore require the simultaneous measurement of upstream (P01 probe) and downstream (P02 probe) flow conditions and probes having the same (and sufficiently short) response time to eliminate any effect of these oscillations on the loss measurements.

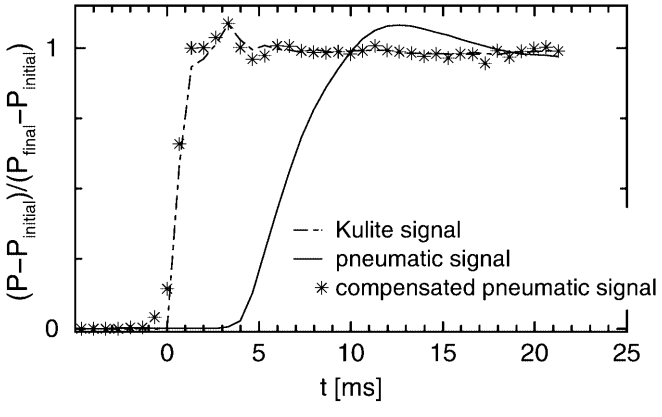

Fig. 7. Reconstruction of the Kulite signal from the slow pneumatic pressure sensor

In this application, both pressure probes have a pressure tubing line and, due to the different tube lengths and differences in the geometry of the probes, a different response is expected.

The dynamic calibration of P01 and P02 probes was performed in a jet exiting a 12-mm-diameter nozzle. Both probes were located 20 mm downstream of the nozzle. A plate situated between the jet nozzle and the probes (≈10 mm downstream of the jet nozzle) deflects the flow. When the plate is rapidly opened both probes are exposed to the same sudden change of pressure. P01 probe reaches the maximum pressure ≈7 ms faster than the P02 probe (see Fig. 8 test 1). It is clear that the slow probe needs some time to notice the pressure step. Data was sampled at 10 kHz. The time delay is $T_d = 1.8$ ms, therefore, $d = 18$ samples. Once d is determined, several orders are investigated using the data from test 1 and Eq. 5. In this case, a fourth-order system produces the best approximation, hence, the transfer function between the P01 probe response and the P02 probe response, is modelled with only nine parameters plus the order m and the delay d. Using $\hat{\Theta}$ from test 1 and Eq. 7, the signals $\hat{u}_N$ are reconstructed for all the four tests. This is done to check if the parameters found in one test can be used in other tests to compensate the slow P02 probe signal and obtain the P01 signal. For all the tests, a satisfactory agreement is observed between the compensated signal and the faster P01 signal. These results validate the parameters obtained for this probe.

Once the parameters were found, the digital compensation routine provides the '*true*' pressure P02 for the wake measurement. In Fig. 9, the wake measurements in the isentropic light piston tunnel are shown. Single-point measurements were obtained with the probe fixed in successive positions (not traversing) which are not affected by dynamic errors. When the traversing P02 signal is not compensated (i.e. raw P02 signal), the pressure difference does not show a similar wake over the three pitches that are traversed. Moreover, there is a clear shift in the wake with the raw P02 signal (almost 0.2 pitches), due to the lag in response of the probe. On the other hand, when the P02 signal is compensated, the wake is on top of the single-point measurements and, additionally, three similar wakes can be identified.

3.4
Shock tube dynamic calibration of fast-response probes with sub-surface-mounted pressure sensors

Fast-response probes can be divided into two categories: with surface flush-mounted sensors or with sub-surface-mounted sensors. Probes of the first category have the shortest response time with frequencies up to 250 kHz. However, they are more vulnerable than those of the second category, in which the sensors are mounted inside the probe behind a small opening at distances of 0.2–2 mm behind the outer surface. Such probes, in fact, offer a better protection of the recessed sensors against impact of particles and also allow a higher spatial resolution, because the hole dimension is usually much smaller than the pressure-sensitive diaphragm of the sensors. These advantages are at the cost of significantly reduced frequency response. The resonance frequency of the hole-cavity-sensor arrangement depends on the length, diameter and shape of the hole and the volume of the cavity in front of the sensor.

The effect of hole length and diameter on the output of sub-surface-mounted sensors was investigated systematically in the ONERA shock tube tunnel in Lille (Fig. 10). The operation and calibration of this facility is reported by Sudan and Flodrops (1989). Tests were run with orifice lengths of 0.6 and 1.7 mm for hole diameters from 0.25 to 0.6 mm. The cavity was kept constant in all the tests. The recessed pressure sensor is mounted side by side with a flush-mounted reference sensor in the end-plate of the low-pressure chamber of the shock tube. The pressure transducers used are Kulite XCQ-062.

For these experiments, the data was sampled at 5 MHz. Both signals exhibit pressure oscillations at the mechanical resonance frequency of the sensor. The hole-cavity geometry of the recessed sensor damps the high-frequency content of the pressure oscillations.

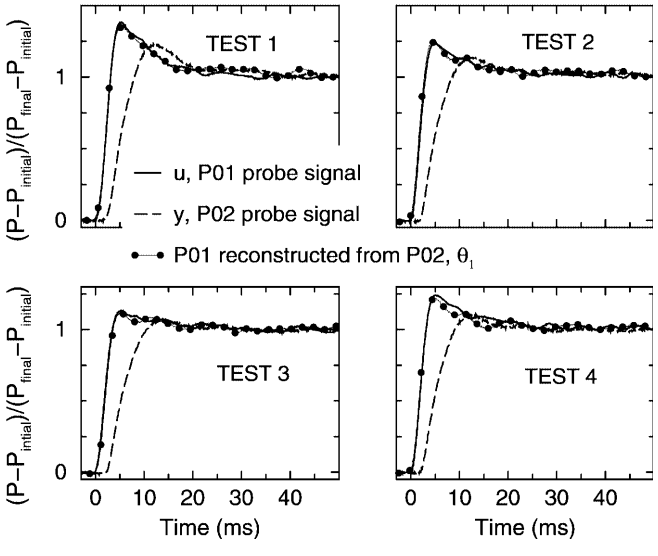

Fig. 8. Several pressure steps and their reconstruction

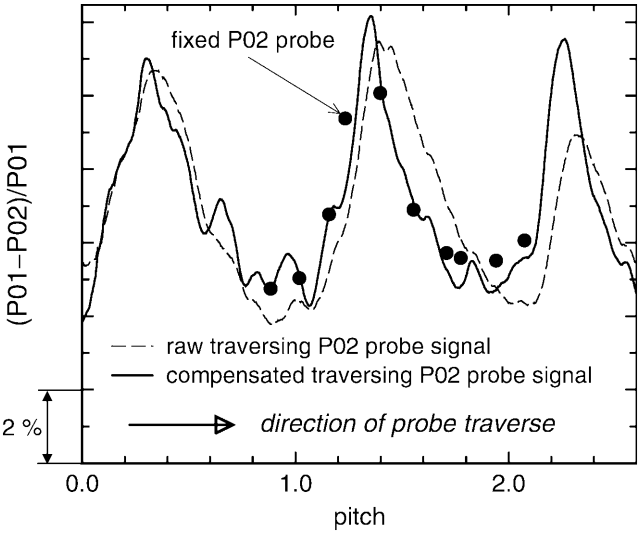

Fig. 9. Wake measurements behind a turbine cascade

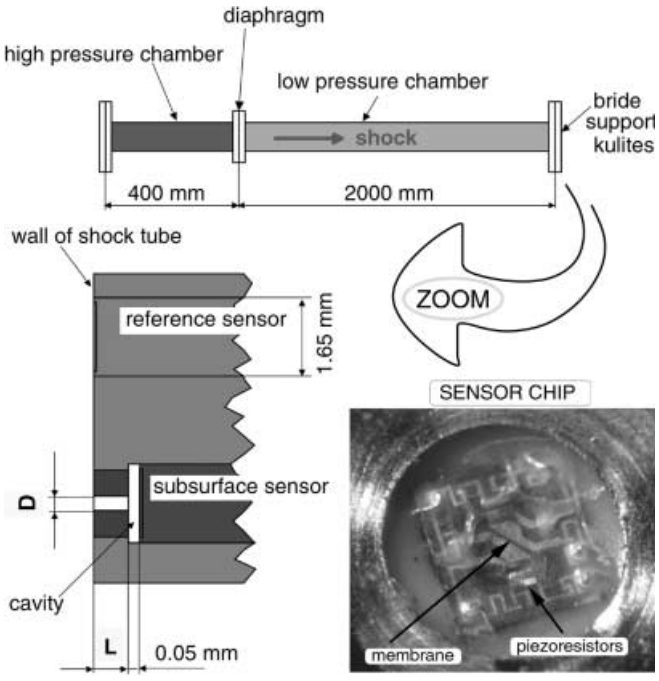

Fig. 10. Shock-tube-testing campaign

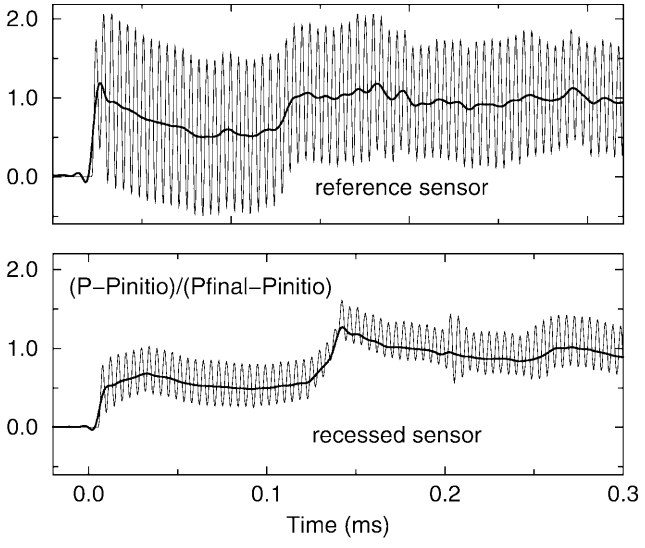

Fig. 11. Step response of the two sensors

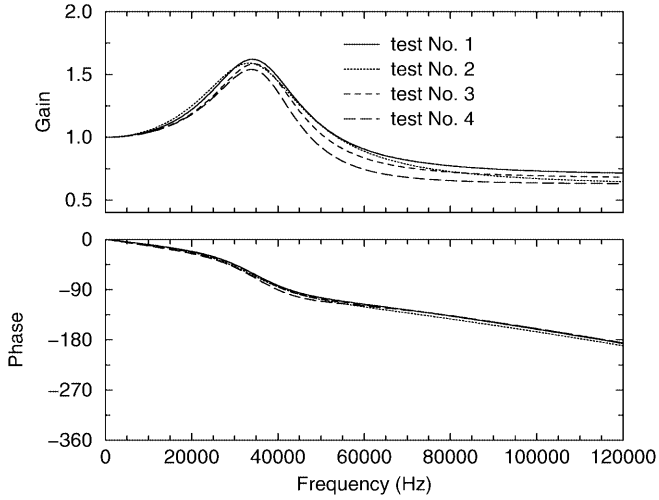

Fig. 12. Repeatability of the transfer function for the configuration with: $L = 1.7$ mm, $\Phi = 0.6$ mm

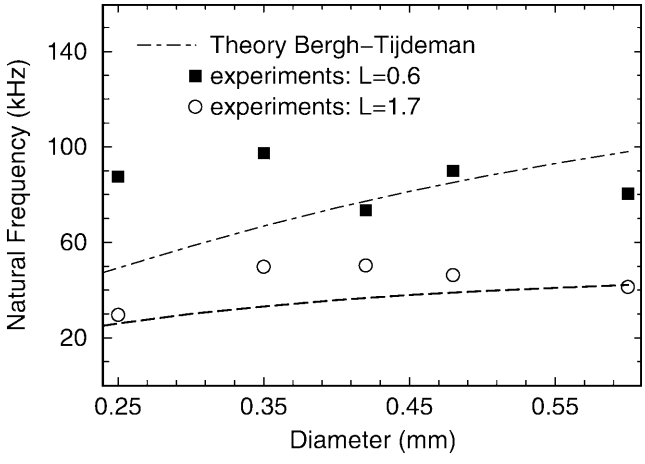

Fig. 13. Natural frequencies of the different configurations

Figure 11 shows the raw and filtered pressure signals for both the reference and the recessed sensor. To determine the digital transfer function, the signal is filtered at 120 kHz, half of the natural frequency of the sensors (≈250 kHz).

Then, using Eq. 5, the parameters of the transfer function are determined. In the present case, the system is modelled with a fourth-order system. Using the set of Eq. 6, the Bode plots are obtained (see Fig. 12). For each of the hole-cavity configurations tested, the resonance frequency was computed. The experimental results are compared with the theoretical results obtained using the theory of Bergh-Tijdeman (1965) in Fig. 13. In general, the theoretical values under-estimate the experimental natural frequency. This is not surprising, because the theory was designed for high L/D ratios. Decreasing L/D, the discrepancy between the experimental and the theoretical results increases. For the case with the smallest orifice length, the natural frequency seems to be independent of the diameter in the range 0.25 –0.6 mm (≈80 kHz), probably because the viscous effects are negligible.

4 Conclusions

The primary outcome of the presented research is the development of an innovative technique to identify the digital transfer function of a digital system, such as the measurement chain commonly used to measure pressure in unsteady flows. The technique models the response of the measurement chain as a linear system of m-order and uses a direct least squares method to identify the $2m+1$ parameters. Because this technique is better suited for step-test analysis than for non-parametric models such as FFT, its use is recommended whenever the transfer function is to be determined from step testing.

An original dynamic calibration using balloon explosions was used successfully. The determination of the transfer function was performed for two line diameters and lengths ranging between 0.1–1.0 m. The numerical system allows to enlarge the frequency bandwidth of the measurement system more than three times.

The applicability of the method was also demonstrated when measuring with a traversing system downstream of a cascade in a blowdown wind tunnel. The frequency response of the downstream probe was enhanced at the level of the upstream probe.

Finally, the transfer function of fast-response probes with sub-surface-mounted sensors was identified. This allows removing the resonance frequency of the hole-cavity geometry, doubling the frequency bandwidth.

Appendix

$$\begin{bmatrix} y_{m+d+1} \\ y_{m+d+2} \\ y_{m+d+3} \\ \vdots \\ y_{m+d+j} \\ \vdots \\ y_N \end{bmatrix} = \begin{bmatrix} -y_{m+d} & -_{m+d-1} & \cdots & -y_{d+1} & u_{m+1} & \cdots & u_1 \\ -y_{m+d+1} & -y_{m+d} & \cdots & -y_{d+2} & u_{m+2} & \cdots & u_2 \\ -y_{m+d+2} & -y_{m+d+1} & \cdots & -y_{d+3} & u_{m+3} & \cdots & u_3 \\ \vdots & \vdots & \vdots & \vdots & \vdots & \vdots & \vdots \\ -y_{m+d+j-1} & -y_{m+d+j-2} & \cdots & -y_{d+j} & u_{m+j} & \cdots & u_j \\ \vdots & \vdots & \vdots & \vdots & \vdots & \vdots & \vdots \\ -y_{N-1} & -y_{N-2} & \cdots & -y_{N-m} & u_{N-d} & \cdots & u_{N-m-d} \end{bmatrix} \cdot \begin{bmatrix} \hat{a}_1 \\ \hat{a}_2 \\ \vdots \\ \hat{a}_m \\ \hat{b}_0 \\ \hat{b}_1 \\ \vdots \\ \hat{b}_m \end{bmatrix} + \begin{bmatrix} e_{m+d+1} \\ e_{m+d+2} \\ e_{m+d+3} \\ \vdots \\ e_{m+d+j} \\ \vdots \\ e_N \end{bmatrix}$$

References

Ainsworth RW; Allen JL (1990) Investigating the performance of miniature semi-conductor pressure transducers for use in fast response aerodynamic probes. In: Proc. of 10th symposium on measuring techniques for transonic and supersonic flows in cascades and turbomachines, 1990, Brussels, Belgium

Bergh H; Tijdeman H (1965) Theoretical and experimental results for the dynamic response of pressure measuring systems. NLR-TR-F.238

Boer RG (1988) Boundary layer effects in unsteady pressure measurements with tubes. NLR TR 88178 U

Bohn D; Schnittfeld T (1992) The dynamic response of capillary tubes for use in miniature pressure probes. In: Proc. of the 11th symposium on measuring techniques for transonic and supersonic flow in cascades and turbomachines, Munich, Germany

Canuto C; Hussaini MY; Quarteroni A; Zang TA (1991) Spectral methods in fluid dynamics. Springer, Berlin Heidelberg New York

Ciocan GD; Baudin J; Vonnez F; Kueny JL (1998) Unsteady five sensors probe development for hydraulic machinery. In: Proc. of ASME fluids engineering summer meeting, 21–25 June, Washington D.C.

Coats JW; Penko PP; Reshotko M (1977) Instrument measures dynamic pressure fluctuations. Nasa technical brief, Lew-12808. Lewis Research Center, Cleveland, Ohio

Dibelius G; Minten G (1983) Measurements of unsteady pressure fluctuations using capillary tubes. In: Proc. of the 7th symposium on measuring techniques for transonic and supersonic flow in cascades and turbomachines, 1983, Aachen, Germany

Dénos R; Sieverding CH (1997) Assessment of the cold-wire resistance thermometer for high-speed turbomachinery applications. J Turbomach 119: 140–148

Etter DM (1981) Adaptive estimation of time delays. In: Proceedings of the international conference on digital signal processing 05.6–09, 1981, Florence, Italy

Gossweiler C (1993) Sonden und Messystem fur schnelle aerodynamische Strömungsmessung mit piezoresistiven Druckgebern. Ph.D. Thesis No. 10253. ETH, Zurich, Switzerland

Gossweiler C; Humm HJ; Kupferschmied P (1990) The use of piezo resistive semi-conductor pressure transducers for fast-response probe measurements in turbomachinery. In: Proc. of 10th symposium on measuring techniques for transonic and supersonic flows in cascades and turbomachines, 1990, Brussels, Belgium

Issermann R (1981) Digital control systems. Springer, Berlin Heidelberg New York

Pallant RJ (1966) A note on the design and construction of a low-pressure calibrator and a comparison with shock tube and static calibration methods. RAE Tech. Report TR 66110

Popp O (1999) Steady and unsteady heat transfer in a film-cooled transonic turbine cascade. Appendix B. Ph.D. Thesis. Virginia Polytechnic Institute and State University

Press WH; Flannery BP; Teukolsky SA; Vetterling WT (1986) Numerical recipes: The art of scientific computing. Cambridge University Press, Cambridge

Redionitis OK; Pathak MM (1999) Simple technique for frequency response enhancement of miniature pressure probes. AIAA J 37

Schweppe JL; Eichberger LC; Muster DF; Michaels EL; Paskusz GF (1963) Methods for the dynamic calibration of pressure transducers. NBS Monograph 67. National Bureau of Standards

Sudan F; Flodrops JP (1989) Etude et realisation d'un banc detalonnage de capteurs de pression. Operation IMFL No. 8336. Onera Report No. 81/11 12 03 81. Onera, Lille, France

Warshawsky I (1991) Lag compensation of optical fibres or thermocouples to achieve waveform fidelity in dynamic gas pyrometry. Rev Sci Instrum 62

Weyer H; Schodl R (1971) Development and testing of techniques for oscillating pressure measurements especially suitable for experimental work in turbomachinery. J Basic Eng